

## Nanospace Engineering of Metal–Organic Frameworks for Adsorptive Gas Separation

Lingshan Gong,<sup>§</sup> Shyam Chand Pal,<sup>§</sup> Yingxiang Ye,<sup>\*</sup> and Shengqian Ma<sup>\*</sup>

Cite This: <https://doi.org/10.1021/accountsmr.5c00006>

Read Online

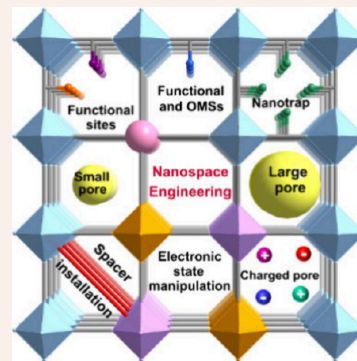
ACCESS |

Metrics & More

Article Recommendations

**CONSPPECTUS:** Gas separation is a critical process in the industrial production of chemicals, polymers, plastics, and fuels, which traditionally rely on energy-intensive cryogenic distillation techniques. In contrast, adsorptive separation using porous materials has emerged as a promising alternative, presenting substantial potential for energy savings and improved operational efficiency. Among these materials, metal–organic frameworks (MOFs) have garnered considerable attention due to their unique structural and functional characteristics. MOFs are a class of crystalline porous materials constructed from inorganic metal ions or clusters connected by organic linkers through strong coordination bonds. Their precisely engineered architectures create well-defined nanoscale spaces capable of selectively trapping guest molecules. In contrast to traditional porous materials such as zeolites and activated carbons, emerging MOFs not only demonstrate exceptional capabilities for pore regulation and interior modification through nanospace engineering but also hold great promise as a superior platform for the development of high-performance functional materials. By virtue of the isorecticular principle and building unit assembly strategies in MOF chemistry, precise adjustments to pore structures—including pore size, shape, and surface chemistry—can be readily achieved, making them well-suited for addressing the separation of intractable industrial gas mixtures, particularly those with similar sizes and physicochemical properties.

This Account presents a comprehensive overview of our recent advancements in high-performance gas separation through nanospace engineering within porous MOFs. First, by strategically immobilizing open metal sites (e.g.,  $\text{Ag}^+$ ) in the pore surface, the functionalized PAF-1- $\text{SO}_3\text{Ag}$  demonstrates enhanced ethylene uptake capacity while maintaining exceptional structural stability under humid conditions. Furthermore, pore surface modification with low-polarity groups (e.g.,  $-\text{CH}_3$ ,  $-\text{CF}_3$ ), as demonstrated in  $\text{Ni}(\text{TMBDC})(\text{DABCO})_{0.5}$ , leads to enhanced  $\text{C}_2\text{H}_6/\text{C}_2\text{H}_4$  separation performance. To achieve strong guest molecule binding, we engineered novel “nanotrap” binding sites that synergistically integrate oppositely adjacent open metal sites and dense alkyl groups, as exemplified by the Cu-ATC framework. Remarkably, Cu-ATC achieves efficient separation of several challenging gas mixtures, including acetylene/carbon dioxide ( $\text{C}_2\text{H}_2/\text{CO}_2$ ), xenon/krypton ( $\text{Xe}/\text{Kr}$ ), and methane/nitrogen ( $\text{CH}_4/\text{N}_2$ ). These innovations have resulted in the development of MOF materials with exceptional separation performance, tailored for specific industrial applications such as light hydrocarbon purification, rare gas separation, and coalbed methane enrichment. Our work not only advances the fundamental understanding of structure–property relationships in MOFs but also provides practical insights for the development of next-generation separation technologies. These advancements hold promise for drastically reducing energy consumption and operational costs in gas separation processes, contributing to more sustainable industrial practices. Future research on MOF materials is anticipated to play a pivotal role in addressing global energy challenges and advancing separation science.



### 1. INTRODUCTION

Separation and purification are critical processes in the modern chemical industry, enabling the extraction of pure or purer components from chemical mixtures for the production of bulk chemical commodities such as plastics, polymers, and fuels.<sup>1–3</sup> Traditional chemical separation technologies that rely on distillation or liquid absorbents are highly energy- and capital-intensive, accounting for 10–15% of global energy consumption.<sup>4</sup> In contrast to those traditional thermal-driven gas separation techniques, emerging adsorbent-based methods, such as pressure swing adsorption, temperature swing adsorption, and membrane technologies, have garnered increasing interest because of their superior energy efficiency

and cost-effectiveness.<sup>5</sup> These nonthermal-driven technologies use chemical affinities or molecular sizes to separate the gas molecules rather than relying on their boiling point differences. As a result, they can be implemented under mild conditions, significantly reducing energy inputs.<sup>6</sup> Solid adsorbents or

**Received:** January 5, 2025

**Revised:** February 27, 2025

**Accepted:** March 18, 2025

Table 1. Nanospace Engineering Enables High Performance Gas Separation

| Adsorbents                      | Strategies   | Mixtures   | Achieved performance  | Ref |
|---------------------------------|--|--|---|-----|
| PAF-1-SO <sub>3</sub> Ag        | Incorporating open Ag(I) sites   | C <sub>2</sub> H <sub>4</sub> /<br>C <sub>2</sub> H <sub>6</sub> | Excellent C <sub>2</sub> H <sub>4</sub> /C <sub>2</sub> H <sub>6</sub> selectivity (27), high C <sub>2</sub> H <sub>4</sub> uptake capacity (91 cm <sup>3</sup> g <sup>-1</sup> ) and Q <sub>st</sub> value (106 kJ mol <sup>-1</sup> ) | 33  |
| MIL-101-Cr-SO <sub>3</sub> Ag   | Incorporating open Ag(I) and Cr(III) functional sites                              | C <sub>2</sub> H <sub>4</sub> /<br>C <sub>2</sub> H <sub>6</sub> | High C <sub>2</sub> H <sub>4</sub> /C <sub>2</sub> H <sub>6</sub> selectivity (9.7, 318 K)  | 34  |
| Ni-MOF-2                        | Optimizing pore size and nonpolar surface  | C <sub>2</sub> H <sub>6</sub> /<br>C <sub>2</sub> H <sub>4</sub> | Excellent C <sub>2</sub> H <sub>6</sub> /C <sub>2</sub> H <sub>4</sub> separation potential (1.7 mmol g <sup>-1</sup> ) and high dynamic C <sub>2</sub> H <sub>4</sub> productivity (12 L kg <sup>-1</sup> )                            | 35  |
| LIFM-63                         | Dynamic spacer installation (optimizing pore size and surface)                     | C <sub>2</sub> H <sub>6</sub> /<br>C <sub>2</sub> H <sub>4</sub> | High C <sub>2</sub> H <sub>6</sub> uptake capacity (3.0 mmol g <sup>-1</sup> ) and moderate C <sub>2</sub> H <sub>6</sub> /C <sub>2</sub> H <sub>4</sub> selectivity (1.56)   | 36  |
| Ni(TMBDC)(DABCO) <sub>0.5</sub> | Optimizing pore size and nonpolar surface  | C <sub>2</sub> H <sub>6</sub> /<br>C <sub>2</sub> H <sub>4</sub> | Unprecedented C <sub>2</sub> H <sub>6</sub> uptake at low pressure (2.21 mmol g <sup>-1</sup> at 0.0625 bar), and high C <sub>2</sub> H <sub>6</sub> /C <sub>2</sub> H <sub>4</sub> selectivity (1.985)                                 | 37  |
| MIL-160                         | Incorporating hydrogen bonding nanotrap sites                                      | C <sub>2</sub> H <sub>2</sub> /<br>CO <sub>2</sub>               | Excellent C <sub>2</sub> H <sub>2</sub> storage capacity (191 cm <sup>3</sup> g <sup>-1</sup> /213 cm <sup>3</sup> cm <sup>-3</sup> ) and dynamic productivity (6.8 mol kg <sup>-1</sup> )  | 38  |
| LIFM-26                         | Incorporating electron rich open Fe(II) sites                                      | C <sub>2</sub> H <sub>2</sub> /<br>CO <sub>2</sub>               | High C <sub>2</sub> H <sub>2</sub> uptake capacity (131 cm <sup>3</sup> g <sup>-1</sup> ) and dynamic productivity (60.0 cm <sup>3</sup> g <sup>-1</sup> )  | 39  |
| FJUT-1                          | Isorecticular contraction (optimizing pore size and surface)                       | C <sub>2</sub> H <sub>2</sub> /<br>CO <sub>2</sub>               | High C <sub>2</sub> H <sub>2</sub> uptake capacity (133.2 cm <sup>3</sup> g <sup>-1</sup> ) and separation factor (5.17)  | 40  |
| FJU-55                          | Optimizing pore size and charged pore surface                                      | Xe/Kr  | High Q <sub>st</sub> value (39.4 kJ mol <sup>-1</sup> ) and superior Xe/Kr selectivity (10)   | 41  |
| ATC-Cu                          | Incorporating nanotrap binding sites (optimizing pore geometry, size, and surface) | CH <sub>4</sub> /N <sub>2</sub>                                  | Unprecedented CH <sub>4</sub> uptake capacity (2.90 mmol g <sup>-1</sup> ) and superior adsorption selectivity (9.7)  | 42  |
|                                 |  | C <sub>2</sub> H <sub>2</sub> /<br>CO <sub>2</sub>               | Excellent low pressure C <sub>2</sub> H <sub>2</sub> uptake (2.1 mmol g <sup>-1</sup> , 1 × 10 <sup>-3</sup> bar) and benchmark C <sub>2</sub> H <sub>2</sub> /CO <sub>2</sub> selectivity (53.6)                                       | 43  |
|                                 |  | Xe/Kr  | Record Xe uptake (2.65 mmol g <sup>-1</sup> , 0.1 bar) and excellent Xe and Kr dynamic capture capacity (32 and 8 mmol kg <sup>-1</sup> )   | 44  |

permeable membranes are central to these emerging technologies, typically made of porous materials containing nanoscale voids, and their effectiveness and efficiency primarily depend on the separation performance of these porous media.

Traditional porous materials, such as zeolites and activated carbon, due to their operational simplicity and significant energy savings, have been widely utilized as adsorbents in various industrial applications, including filtration, separation, purification, and drying.<sup>7</sup> However, the limitations of these established porous adsorbents in precisely controlling pore structures restrict their separation efficiency, particularly in challenging gas separations involving molecules with highly similar physical and chemical properties. Therefore, there is an urgent need to develop advanced porous materials that feature a precisely controllable pore structure to meet the increasing demands for efficient separation.

Over the past two decades, a special type of crystalline porous framework materials, metal–organic frameworks (MOFs, also known as porous coordination polymers),<sup>8,9</sup> featuring exceptional porosity, high modularity, and abundant functionality, has garnered extensive attention from the worldwide communities in chemistry, engineering, and materials science.<sup>10,11</sup> They can be easily obtained by assembling metal ions or clusters with organic linkers via coordination bonds, and their potential applications span a wide range of fields, including gas storage and separation, sensing, biomedicine, and catalysis.<sup>12–21</sup> The strategy of integrating well-defined organic linkers with diverse functionalities and metal-containing nodes has resulted in the synthesis of numerous novel porous materials exhibiting unique and tunable properties. Ascribe to the isorecticular principle in MOF chemistry, valuable insights are provided that facilitate the design of tailor-made porous materials via building block assembly. Moreover, the easily achieved postsynthetic modifications also facilitate the development of metal–organic frameworks.<sup>9,22</sup> Particularly, the definite single-crystal structure of MOFs provides a preeminent platform for exploring the interaction mechanisms of gas molecules in nanoconfined space (or nanotraps),<sup>23,24</sup> which can promote the design and

syntheses of novel porous media for efficient separation. In this context, a growing number of MOFs with ascendant performance through precise pore regulation and interior modification have been designed to settle the separation of numerous challenging yet crucial gas mixtures (e.g., alkyne/alkene,<sup>25,26</sup> olefin/paraffin<sup>27–32</sup>).

This Account highlights our endeavors in advancing the nanospace engineering of MOFs for enhanced adsorptive gas separation. Two complementary strategies have been developed to precisely regulate pore architectures: (1) pore surface functionalization through the strategic incorporation of open metal sites (OMSs), nanotrap binding sites, low-polarity functional groups (–CH<sub>3</sub>, –CF<sub>3</sub>, aromatic rings), and the construction of ionic frameworks; and (2) simultaneous optimization of pore sizes and surface chemistry via isorecticular contraction and dynamic spacer installation techniques. As demonstrated in Table 1, we achieved top-performing microporous MOF materials through these approaches for the separation of critical gas mixtures, including C<sub>2</sub>H<sub>4</sub>/C<sub>2</sub>H<sub>6</sub>, C<sub>2</sub>H<sub>2</sub>/CO<sub>2</sub>, CH<sub>4</sub>/N<sub>2</sub>, and Xe/Kr. Finally, we present our perspective on future opportunities and significant challenges associated with porous materials for practical applications in gas separation.

## 2. NANOSPACE ENGINEERING FOR ENHANCED GAS ADSORPTION AND SEPARATION

### 2.1. Incorporating Open Metal Sites for C<sub>2</sub>H<sub>4</sub>/C<sub>2</sub>H<sub>6</sub> Separation

Ethylene (C<sub>2</sub>H<sub>4</sub>) is one of the most crucial feedstocks in the petrochemical industry used to produce valuable commodities that are extensively utilized in the packaging, automobile, and electrical industries.<sup>45</sup> The massive demand for high-purity ethylene (≥99.5%) feedstock is mainly met through the steam cracking of naphtha or ethane (C<sub>2</sub>H<sub>6</sub>), followed by purification using cryogenic distillation technology to eliminate impurities such as C<sub>2</sub>H<sub>6</sub>. In comparison to traditional thermally driven separation technologies, emerging adsorptive separation

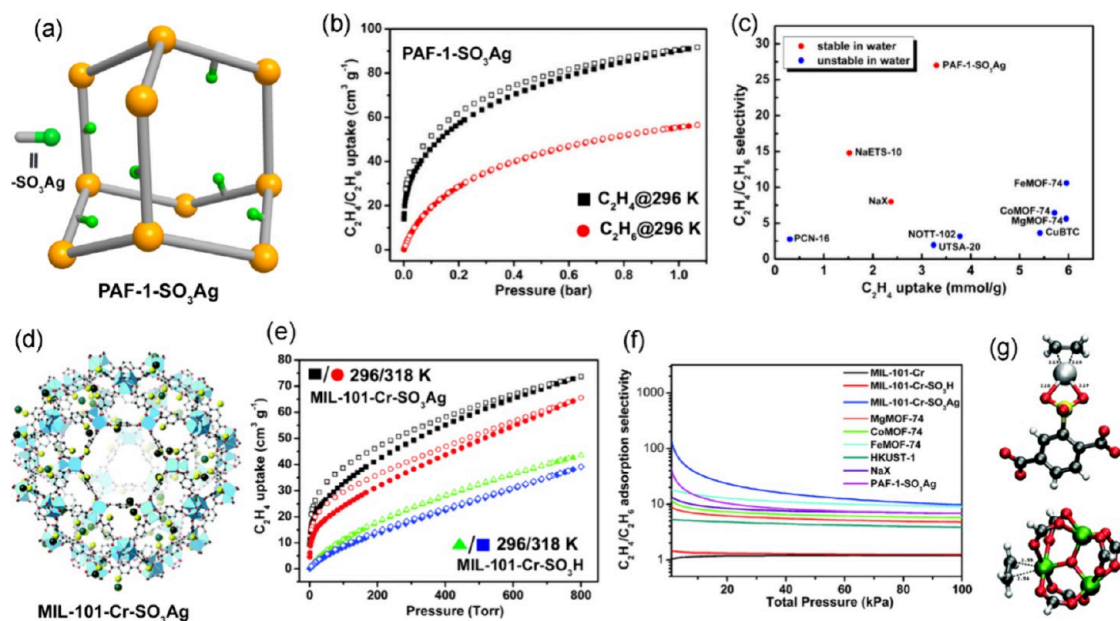


**Figure 1.** (a) Structural diagram of PAF-1-SO<sub>3</sub>Ag. (b, c) C<sub>2</sub>H<sub>4</sub>–C<sub>2</sub>H<sub>6</sub> adsorption isotherms and separation performance of PAF-1-SO<sub>3</sub>Ag. Reproduced with permission from ref 33. Copyright 2014 American Chemical Society. (d) Crystal structure of MIL-101-Cr-SO<sub>3</sub>Ag. (e) C<sub>2</sub>H<sub>4</sub> adsorption isotherms at different temperatures. (f) Selectivity comparison of C<sub>2</sub>H<sub>4</sub> selective adsorbents. (g) C<sub>2</sub>H<sub>4</sub> binding mechanism investigated by DFT simulation. Reproduced with permission from ref 34. Copyright 2015 Royal Society of Chemistry.

methods have garnered attention for their potential to achieve highly energy-efficient separations with low carbon footprints.

Olefin/paraffin separation primarily relies on the selective adsorption of olefin through reversible  $\pi$ -complexation with the open metal centers (either with intrinsic open metal sites, or extrinsically loaded Cu<sup>I</sup>/Ag<sup>I</sup> metal ions).<sup>27,46</sup> However, MOFs with intrinsic OMSs usually suffer from compromised stability, particularly under moist conditions, which hinders their practical applications. To address this challenge, we pioneered a nanospace engineering strategy in 2014 by integrating functional sites (–SO<sub>3</sub>Ag) into the nonpolar backbone of a highly chemically stable porous aromatic framework (PAF-1). Notably, the functionalized porous aromatic framework (PAF-1-SO<sub>3</sub>Ag) not only significantly enhances the ethylene uptake capacity but also maintains structural stability under water/humid atmosphere, effectively overcoming the pressing stability issues encountered by certain OMS-containing MOFs (Figure 1a–c).<sup>33</sup> At 296 K and 1 atm, PAF-1-SO<sub>3</sub>Ag exhibits a C<sub>2</sub>H<sub>4</sub> uptake of 4.1 mmol g<sup>–1</sup>, which is slightly lower than that of porous MOFs with a high-density OMS, such as Mg-MOF-74 (7.2 mmol g<sup>–1</sup>), Cu-BTC (7.2 mmol g<sup>–1</sup>), and NOTT-102 (5.8 mmol g<sup>–1</sup>). However, this uptake significantly surpasses that of the widely studied zeolite 5A (~2.3 mmol g<sup>–1</sup> at 303 K) and is comparable to that of zeolite NaX (4.2 mmol g<sup>–1</sup> at 305 K). The strong  $\pi$ -complexation was confirmed through *in situ* IR spectroscopy studies, revealing the highest C<sub>2</sub>H<sub>4</sub> binding energy (106 kJ mol<sup>–1</sup>) and an exceptional C<sub>2</sub>H<sub>4</sub>/C<sub>2</sub>H<sub>6</sub> selectivity (27), significantly surpassing that of FeMOF-74 (13.6), CoMOF-74 (6), MnMOF-74 (8), and CuBTC (4). Moreover, transient simulations and laboratory-scale dynamic breakthrough experiments both indicated that the 50:50 (v/v) C<sub>2</sub>H<sub>4</sub>/C<sub>2</sub>H<sub>6</sub> mixture flowing over the PAF-1-SO<sub>3</sub>Ag packed column can be efficiently separated. It is possible to recover polymer grade ethylene by a pressure swing adsorption operation in PAF-1-SO<sub>3</sub>Ag.

The separation of C<sub>2</sub>H<sub>4</sub>/C<sub>2</sub>H<sub>6</sub> at higher temperatures may require more substantial binding sites due to the weak and reversible nature of alone  $\pi$ -complexation. To address this and further verify the universality of the aforementioned strategy, a synergistic integration of OMSs and  $\pi$ -complexation has been achieved in a highly stable sulfonic acid-functionalized MOF (MIL-101-Cr-SO<sub>3</sub>Ag, Figure 1d–h).<sup>34</sup> At 318 K, the ethylene uptake capacity of MIL-101-Cr-SO<sub>3</sub>Ag (63 cm<sup>3</sup> g<sup>–1</sup>) surpasses the pristine MIL-101-Cr-SO<sub>3</sub>H (37 cm<sup>3</sup> g<sup>–1</sup>), despite having a lower surface area. The significant improvement of the C<sub>2</sub>H<sub>4</sub> binding interaction was evident from the remarkably higher  $Q_{st}$  of 63 kJ mol<sup>–1</sup> in MIL-101-Cr-SO<sub>3</sub>Ag, compared to 10 kJ mol<sup>–1</sup> in MIL-101-Cr-SO<sub>3</sub>H, highlighting the cooperative role of open Cr(III) and Ag(I) sites. The selectivity for the equimolar C<sub>2</sub>H<sub>4</sub>/C<sub>2</sub>H<sub>6</sub> mixtures is 9.7 (at 318 K under 100 kPa), which is much higher than that of MIL-101-Cr-SO<sub>3</sub>H (1.2) and even surpasses the previously developed PAF-1-SO<sub>3</sub>Ag (7), and other benchmark materials such as NaX (6.8), CoMOF-74 (5.7), and CuBTC (3.8). The synergistic mechanism for ethylene capture was further validated through *in situ* IR spectroscopic studies and theoretical calculations. Although a highly efficient C<sub>2</sub>H<sub>4</sub> separation performance can be achieved by introducing functional OMSs, the high energy consumption required for regeneration may pose a great barrier to the practical implementation of C<sub>2</sub>H<sub>4</sub>-selective materials.

## 2.2. Constructing Nonpolar Pore Surfaces for C<sub>2</sub>H<sub>6</sub>/C<sub>2</sub>H<sub>4</sub> Separation

Compared to well-explored ethylene-selective porous materials, the use of ethane-selective materials represents a more economical process, as it can yield polymer grade ( $\geq 99.5\%$ ) C<sub>2</sub>H<sub>4</sub> in a single operation.<sup>47</sup> However, developing C<sub>2</sub>H<sub>6</sub>-selective MOFs is quite challenging because typical functional sites, particularly OMSs, tend to interact more strongly with C<sub>2</sub>H<sub>4</sub> than with C<sub>2</sub>H<sub>6</sub>. By leveraging the slightly greater polarizability of C<sub>2</sub>H<sub>6</sub> compared to C<sub>2</sub>H<sub>4</sub> ( $44.7 \times 10^{-25}$  cm<sup>3</sup> vs

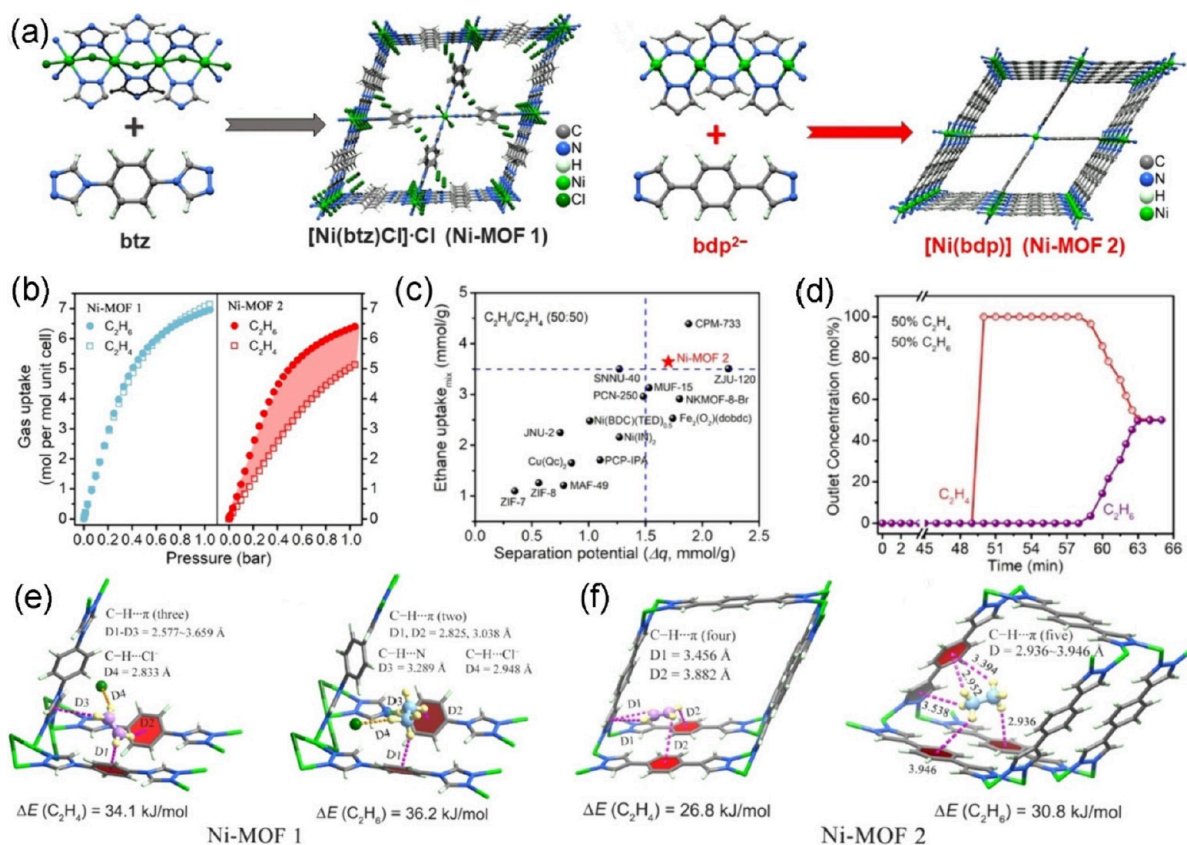


**Figure 2.** (a) Synthesis diagram of Ni-MOF-1 and Ni-MOF-2. (b-d) C<sub>2</sub>H<sub>6</sub> and C<sub>2</sub>H<sub>4</sub> gas adsorption isotherms, separation potential, and dynamic separation performance of Ni-MOF-2. C<sub>2</sub>H<sub>4</sub> and C<sub>2</sub>H<sub>6</sub> binding sites in Ni-MOF-1 (e) and Ni-MOF-2 (f). Reproduced with permission from ref 35. Copyright 2023 Wiley-VCH.

$42.52 \times 10^{-25} \text{ cm}^3$ ), we developed a series of C<sub>2</sub>H<sub>6</sub>-selective MOFs by employing nanospace engineering strategies to construct nonpolar pore surfaces. In 2019, we developed a strategy to create a nonpolar pore surface environment by enriching underutilized functional sites to enhance the binding affinity for C<sub>2</sub>H<sub>6</sub>.<sup>37</sup> In contrast to the prototypical MOF, Ni(BDC)(DABCO)<sub>0.5</sub>, which shows low C<sub>2</sub>H<sub>6</sub> uptake and poor C<sub>2</sub>H<sub>6</sub>/C<sub>2</sub>H<sub>4</sub> selectivity, the methyl fully substituted MOF [Ni(TMBDC)(DABCO)<sub>0.5</sub>] with nonpolar surface and smaller pore channels (5.9 Å) demonstrated higher C<sub>2</sub>H<sub>6</sub> uptake (2.21 mmol g<sup>-1</sup> at 0.0625 bar) and IAST selectivity (1.985). The dynamic breakthrough study utilizing the fully methyl-substituted MOF material, which demonstrated a clean and sharp separation, produced over 99.9% pure C<sub>2</sub>H<sub>4</sub> in a single step.

For C<sub>2</sub>H<sub>6</sub>-selective materials, the overall C<sub>2</sub>H<sub>4</sub> productivity is correlated with a combined metric of gas uptake capacity and separation selectivity rather than considering just a single parameter. In this context, we recently developed two highly porous isoreticular MOFs (named Ni-MOF-1 and Ni-MOF-2, with chemical formula of [Ni(btz)Cl]·Cl and [Ni(bdp)], where btz = 1,4'-bis(4H-1,2,4-triazol-4-yl)benzene and H<sub>2</sub>bdp = 1,4-benzenedipyrazole), constructed from  $\pi$ -conjugated aromatic organic linkers.<sup>35</sup> In contrast to the cationic framework (Ni-MOF-1), which shows almost identical uptake of C<sub>2</sub>H<sub>4</sub> and C<sub>2</sub>H<sub>6</sub>, the neutral framework (Ni-MOF-2) with a rich, accessible nonpolar/inert pore surface and optimized pore shape showed high ethane uptake capacity (133 cm<sup>3</sup> g<sup>-1</sup>) and superior C<sub>2</sub>H<sub>6</sub>/C<sub>2</sub>H<sub>4</sub> selectivity of 1.9 (Figure 2). The preferential adsorption of C<sub>2</sub>H<sub>6</sub> over C<sub>2</sub>H<sub>4</sub> in Ni-MOF-2 was

verified by Q<sub>st</sub> results (C<sub>2</sub>H<sub>6</sub>: 23.6 kJ mol<sup>-1</sup>; C<sub>2</sub>H<sub>4</sub>: 21.4 kJ mol<sup>-1</sup>) and Density Functional Theory (DFT) studies. Importantly, the separation potential ( $\Delta q$ ) of Ni-MOF-2 from a 50:50 C<sub>2</sub>H<sub>6</sub>/C<sub>2</sub>H<sub>4</sub> mixture is as high as 1.7 mmol g<sup>-1</sup>, comparable to the top performing MOFs such as CPM-773 (1.88 mmol g<sup>-1</sup>) and Fe<sub>3</sub>O<sub>2</sub>(dobdc) (1.74 mmol g<sup>-1</sup>), and higher than most of the C<sub>2</sub>H<sub>6</sub> selective materials, making it one of the best porous materials for this critical gas separation. Additionally, dynamic breakthrough experiments further validated the potential of Ni-MOF-2 for high-purity ethylene recovery of up to 12 L kg<sup>-1</sup> in a single operation.

Selective C<sub>2</sub>H<sub>6</sub> separation has been achieved through pore engineering, by either regulating the pore aperture size or modifying the pore surface according to the higher polarizability of C<sub>2</sub>H<sub>6</sub>. However, a systematic strategy for developing a C<sub>2</sub>H<sub>6</sub> selective adsorbent is still lacking in the literature and thus demands particular attention. Recognizing this gap, we developed a dynamic spacer installation (DSI) strategy to create a series of multifunctional MOFs with optimized pore volume and environment to enhance C<sub>2</sub>H<sub>6</sub>/C<sub>2</sub>H<sub>4</sub> separation (Figure 3).<sup>36</sup> In contrast to *proto*-MOF LIFM-28 ([Zr<sub>6</sub>( $\mu_3$ -O)<sub>8</sub>(H<sub>2</sub>O)<sub>8</sub>(L<sup>1</sup>)<sub>4</sub>], L<sup>1</sup> = 2, 2'-bis(trifluoromethyl)-4,4'-biphenyldicarboxylate), the functional spacer installed MOFs, especially LIFM-63 ([Zr<sub>6</sub>O<sub>4</sub>(OH)<sub>4</sub>(L<sup>1</sup>)<sub>4</sub>(L<sup>4</sup>)<sub>1.10</sub>(L<sup>5</sup>)<sub>1.04</sub>], L<sup>4</sup> = biphenyl-4,4'-dicarboxylate, L<sup>5</sup> = 2'-methyl-[1,1':4',1'-terphenyl]-4,4''-dicarboxylate), generated optimized pore surface and pore size showing much higher C<sub>2</sub>H<sub>6</sub> uptake capacity and superior IAST selectivity. The C<sub>2</sub>H<sub>6</sub> uptake of LIFM-63 at 298 K (3.0 mmol g<sup>-1</sup>) is greater than that of MAF-49 (1.70 mmol g<sup>-1</sup>),

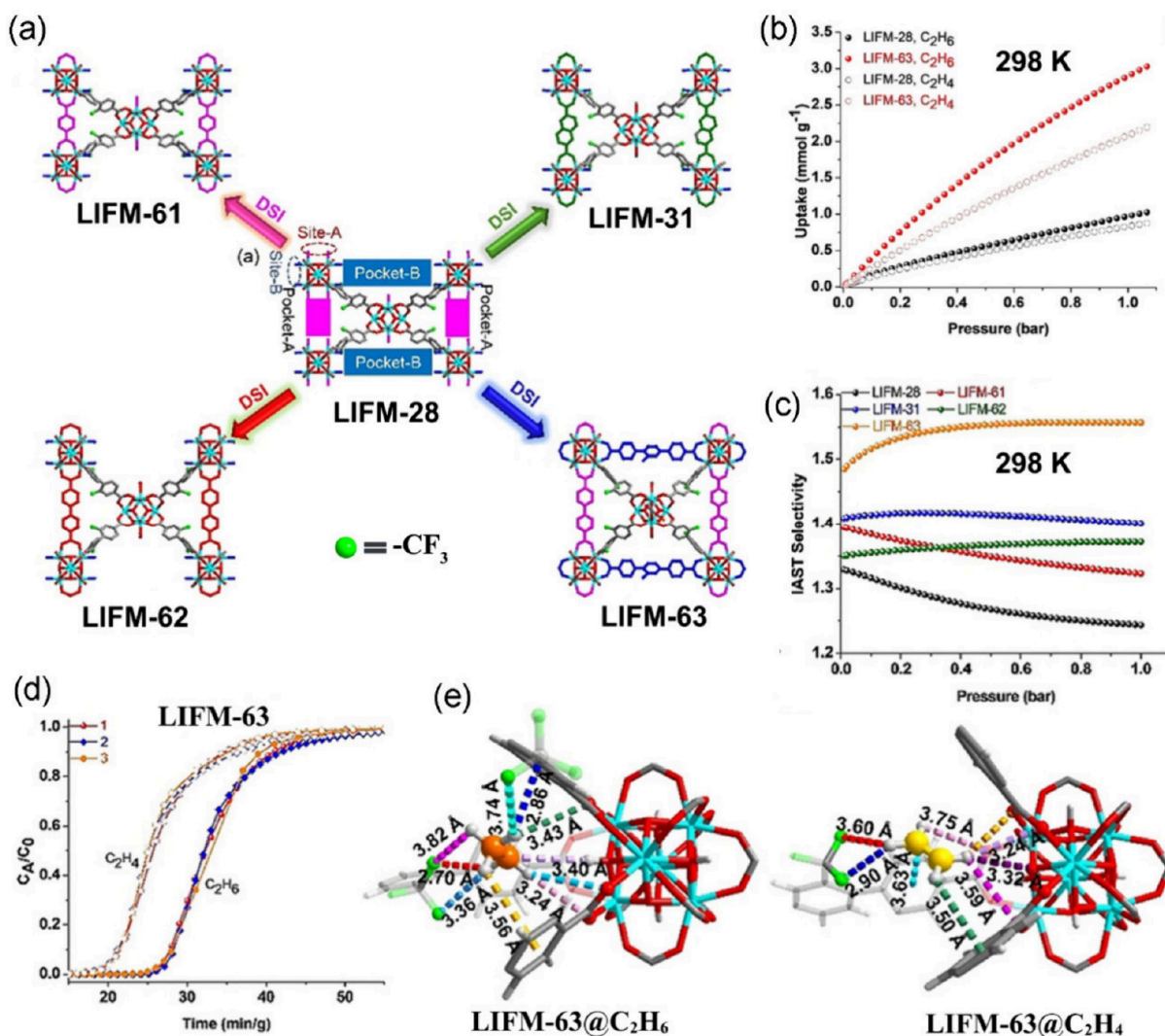


**Figure 3.** (a) Schematic representation of nanospace engineering through dynamic spacer installation. (b)  $\text{C}_2\text{H}_6$  and  $\text{C}_2\text{H}_4$  adsorption isotherms. (c) IAST selective comparison of different MOFs. (d) Dynamic breakthrough curves for LIFM-63. (e) Preferential gas binding sites in LIFM-63. Reproduced with permission from ref 36. Copyright 2021 Wiley-VCH.

ZIF-7 ( $2.24 \text{ mmol g}^{-1}$ ) and Cu(Qc) ( $1.85 \text{ mmol g}^{-1}$ ). This could be attributed to the presence of the dynamic spacers in both Pocket-A and Pocket-B, which create multiple favorable  $\text{C}_2\text{H}_6$  adsorption sites through  $\text{C}-\text{H}\cdots\text{F}$ ,  $\text{C}-\text{H}\cdots\text{O}$  (with the framework), and  $\text{C}-\text{H}\cdots\pi$  (spacers) interactions, resulting from the increased pore surface area and pore volume. On the contrary, in LIFM-31/61/62, the dynamic spacers were present only in Pocket-A, resulting in a much smaller surface area and pore volume. Additionally, the GCMC simulation further revealed a stronger interaction with  $\text{C}_2\text{H}_6$  compared to that with  $\text{C}_2\text{H}_4$ , due to the presence of additional functional sites in LIFM-63. Further, the breakthrough study also indicated that the postsynthetic modification of LIFM-63 could not only produce polymer grade  $\text{C}_2\text{H}_4$  (>99.9%) in a single step but also had good cyclic stability. Consequently, the installation of dynamic linkers may serve as a promising pore engineering strategy for the further development of  $\text{C}_2\text{H}_6$ -selective adsorbents.

### 2.3. Incorporating Nanotraps and Open Metal Sites for $\text{C}_2\text{H}_2/\text{CO}_2$ Separation

$\text{C}_2\text{H}_2$  is a valuable industrial gas primarily utilized as a fuel and as a precursor for various commodity products.<sup>48</sup> Generating

pure  $\text{C}_2\text{H}_2$  necessitates the selective removal of  $\text{CO}_2$ , presenting one of the most formidable separation challenges because of their identical kinetic diameter (3.3 Å) and close boiling points ( $\text{C}_2\text{H}_2$ , 189.3 K;  $\text{CO}_2$ , 194.7 K).<sup>1,7,49,50</sup> Generally, MOFs with OMSs exhibit strong interactions with  $\text{C}_2\text{H}_2$ , facilitating  $\text{C}_2\text{H}_2/\text{CO}_2$  separations. However, these OMSs can also significantly enhance the coadsorption of  $\text{CO}_2$ , thereby reducing separation efficiency. A viable solution to this challenge involves the precise regulation of the pore environment at the subangstrom level through pore engineering, which provides multiple binding sites to enhance interactions with  $\text{C}_2\text{H}_2$ , ultimately achieving efficient  $\text{C}_2\text{H}_2/\text{CO}_2$  separation.

In this context, we developed "nanotrap" binding sites in ATC-Cu ( $[\text{Cu}_2(\text{ATC})]$ , where  $\text{H}_2\text{ATC} = 1,3,5,7$ -adamantane tetracarboxylic acid) for the trace capture and selective separation of  $\text{C}_2\text{H}_2$  from the  $\text{CO}_2$ -containing mixtures.<sup>43</sup> The 3D nanotrap features a sandwich-like binding site (site-I) formed by opposite  $\text{Cu}^{\text{II}}$ -paddlewheel units and an aliphatic hydrogen-rich cavity (site-II). The site-I exhibits a strong Coulombic charge density, creating an ideal environment for highly selective  $\text{C}_2\text{H}_2$  binding (Figure 4), resulting in a sharp

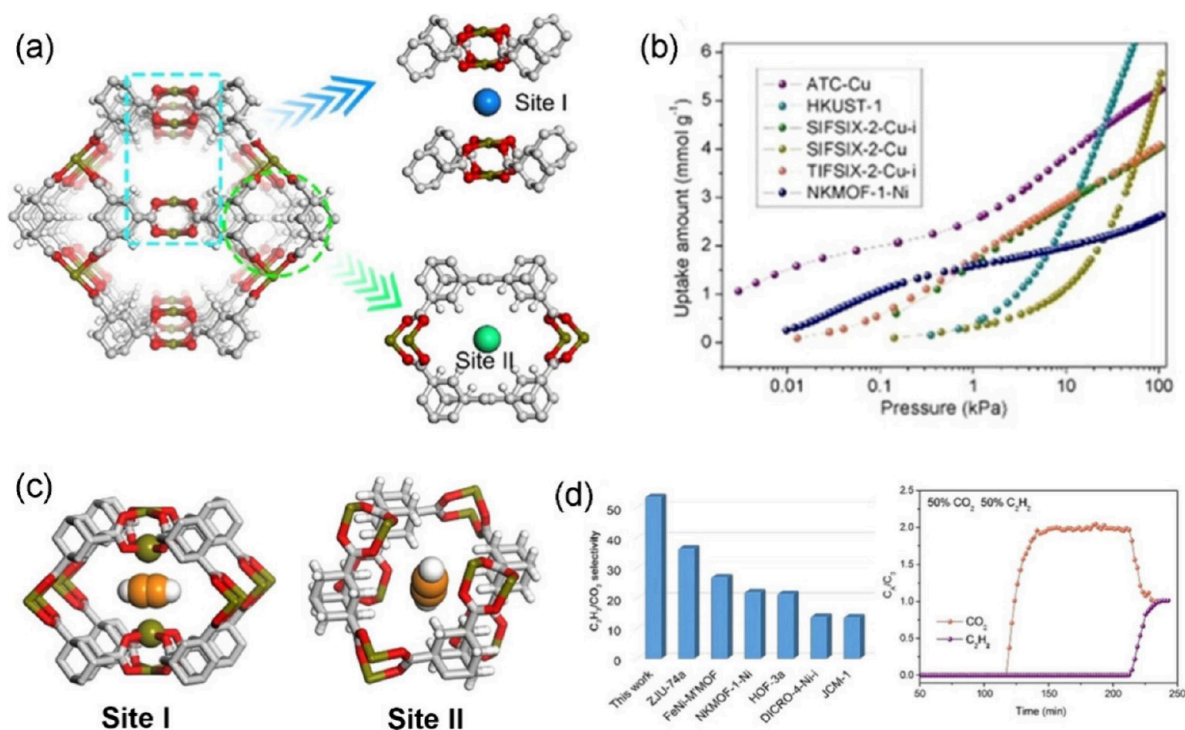


**Figure 4.** (a) Crystal structure of ATC-Cu. (b) Comparison of  $C_2H_2$  adsorption isotherms of top-performance MOFs. (c)  $C_2H_2$  binding location at ultralow pressure (Site I,  $1 \times 10^{-4}$  bar) and ambient pressure (Site II) from single crystal structure. (d) IAST selectivity and dynamic breakthrough curves of ATC-Cu. Reproduced with permission from ref 43. Copyright 2021 Wiley-VCH.

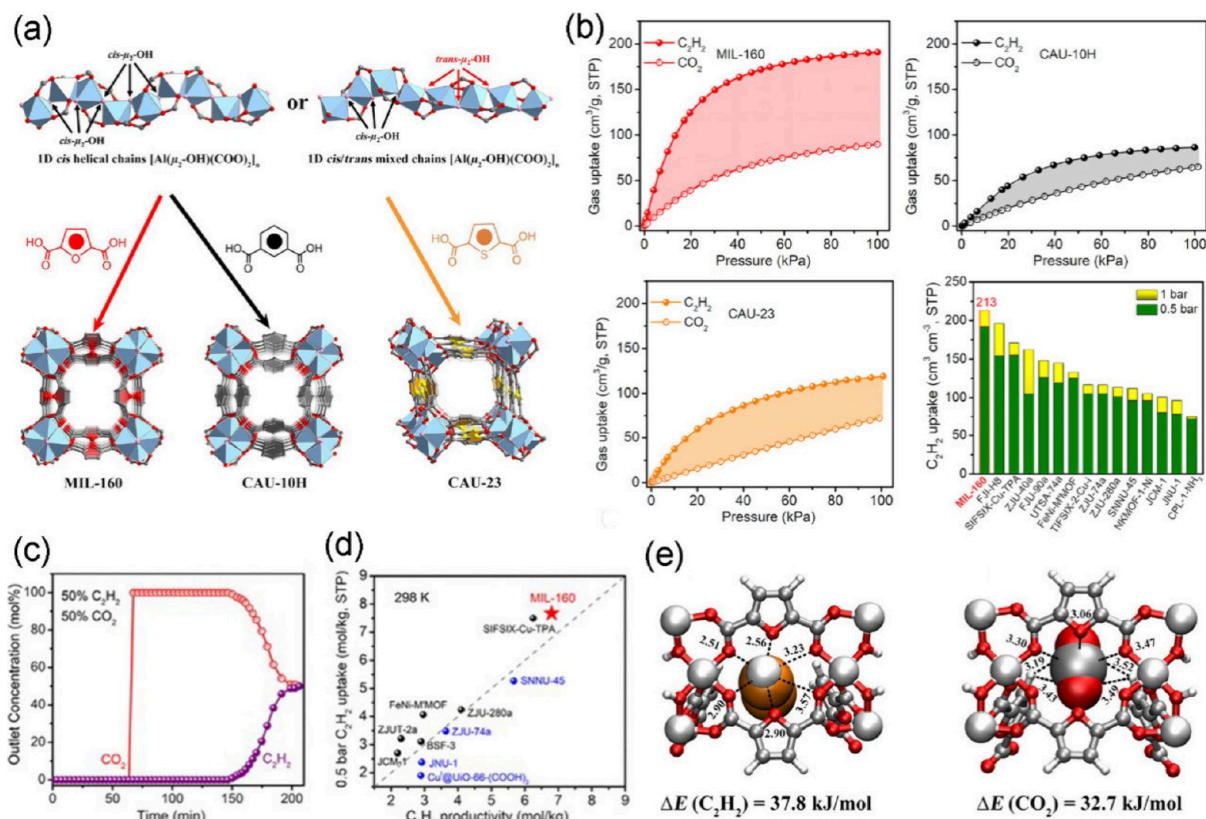


**Figure 5.** (a) Schematic illustration of three isorecticular frameworks. (b) Comparison of  $C_2H_2$  and  $CO_2$  capture performances at 298 K. (c) Dynamic breakthrough separation performance of MIL-160. (d) Comparison of  $C_2H_2$  productivity among the benchmark MOFs. (e) Primary  $C_2H_2$  and  $CO_2$  binding sites in MIL-160. Reproduced with permission from ref 38. Copyright 2022 American Chemical Society.

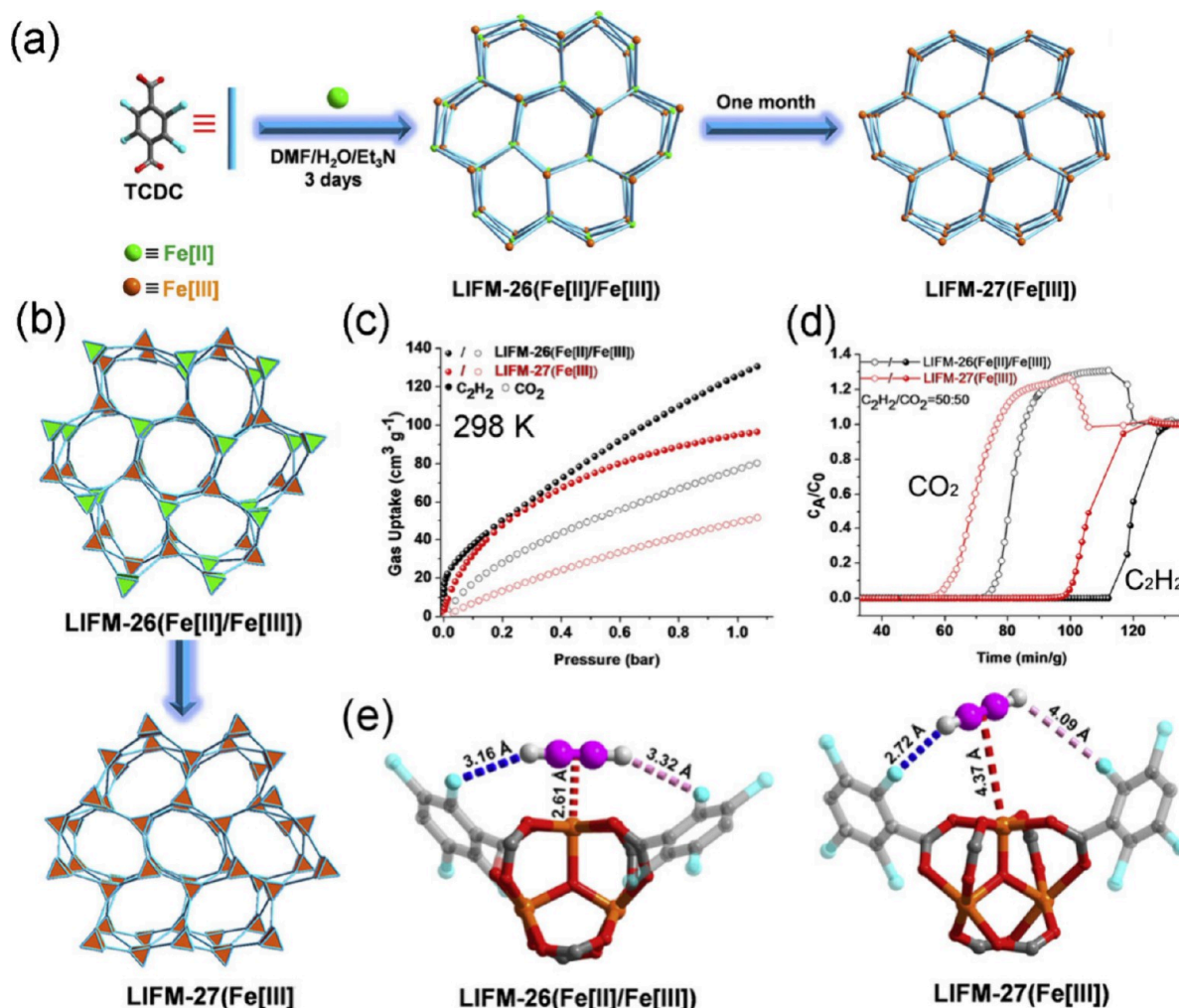


**Figure 6.** (a,b) Schematic synthesis process of the two isostructural Fe-MOFs. (c) C<sub>2</sub>H<sub>2</sub> and CO<sub>2</sub> adsorption isotherms, (d) breakthrough separation performance, and (e) preferred C<sub>2</sub>H<sub>2</sub> adsorption sites of Fe-MOFs. Reproduced with permission from ref 39. Copyright 2022 Elsevier.

C<sub>2</sub>H<sub>2</sub> uptake of 2.1 mmol g<sup>-1</sup> at ultralow pressure (1 × 10<sup>-3</sup> bar), highest among the C<sub>2</sub>H<sub>2</sub>-selective adsorbents. At 298 K and 1 bar, the C<sub>2</sub>H<sub>2</sub> and CO<sub>2</sub> uptakes were 5.01 mmol g<sup>-1</sup> and 4.02 mmol g<sup>-1</sup>, respectively, yielding an ultrahigh C<sub>2</sub>H<sub>2</sub> selectivity of 53.6 for equimolar mixture. The preferential adsorption of C<sub>2</sub>H<sub>2</sub> at Site-I was confirmed through GCMC simulation studies, consistent with the gas-loaded single-crystal structure. A dual coordination interaction at this site resulted in the strongest C<sub>2</sub>H<sub>2</sub> binding energy ( $Q_{st} = 79.1$  kJmol<sup>-1</sup>) among the high-performing C<sub>2</sub>H<sub>2</sub>-selective MOFs. The separation performance of ATC-Cu for C<sub>2</sub>H<sub>2</sub>/CO<sub>2</sub> was further evaluated through dynamic breakthrough experiments, with the results highlighting its significant potential for highly efficient separation. This work achieves one of the best performances in C<sub>2</sub>H<sub>2</sub> capture and C<sub>2</sub>H<sub>2</sub>/CO<sub>2</sub> separation by exploiting the synergistic binding interactions, paving the way for the development of high-performance porous materials for gas separation.

Drawing inspiration from the specific recognition capabilities of crown ether complexes, a hydrogen-bonded nanotrapp grafted onto the pore surfaces of MOFs was developed to efficiently separate the C<sub>2</sub>H<sub>2</sub>/CO<sub>2</sub> mixture. As proof of concept, we have modified the H-bonding nanotrapp on the pore surfaces within three isostructural MOFs, MIL-160, CAU-10H, and CAU-23, based on the principles of reticular

chemistry (Figure 5).<sup>38</sup> Benefiting from the highest density of hydrogen bond receptor nanotraps, MIL-160 exhibits exceptional C<sub>2</sub>H<sub>2</sub> uptake (191 cm<sup>3</sup> g<sup>-1</sup>, or 213 cm<sup>3</sup> cm<sup>-3</sup>) and much less CO<sub>2</sub> adsorption (90 cm<sup>3</sup> g<sup>-1</sup>), with a remarkable C<sub>2</sub>H<sub>2</sub>/CO<sub>2</sub> selectivity of 10. The volumetric C<sub>2</sub>H<sub>2</sub> uptake in MIL-160 (213 cm<sup>3</sup> cm<sup>-3</sup>) is slightly lower than record uptake of OMSs rich Co-MOF-74 (230 cm<sup>3</sup> cm<sup>-3</sup>) and surpassed most of the C<sub>2</sub>H<sub>2</sub>/CO<sub>2</sub> separating benchmark MOFs including FJI-H8 (196 cm<sup>3</sup> cm<sup>-3</sup>), SIFSIX-Cu-TPA (185 cm<sup>3</sup> cm<sup>-3</sup>), FJU-90a (180 cm<sup>3</sup> cm<sup>-3</sup>) and UTSA-74a (108 cm<sup>3</sup> cm<sup>-3</sup>). The *in situ* FT-IR tests and molecular simulations studies further reveal that the unique host-guest interaction between the nanotrapp and C<sub>2</sub>H<sub>2</sub> molecule resulting in one of the highest storage capacities and excellent selectivity. Moreover, both simulated and experimental breakthroughs establish MIL-160 as a new benchmark for separating this challenging gas mixture, achieving an excellent separation potential of 5.02 mol/kg and a dynamic C<sub>2</sub>H<sub>2</sub> productivity of 6.8 mol/kg, respectively.

As previously discussed, the open metal sites in MOFs render a strong affinity for alkynes/alkenes due to the polarizability of  $\pi$ -electrons. Consequently, by changing the oxidation state of the OMSs within MOFs, the selectivity for C<sub>2</sub>H<sub>2</sub> can be fine-tuned. However, synthesizing MOFs that combine a high density of electronically rich OMSs remains challenging and is largely unexplored. In 2022, we reported for

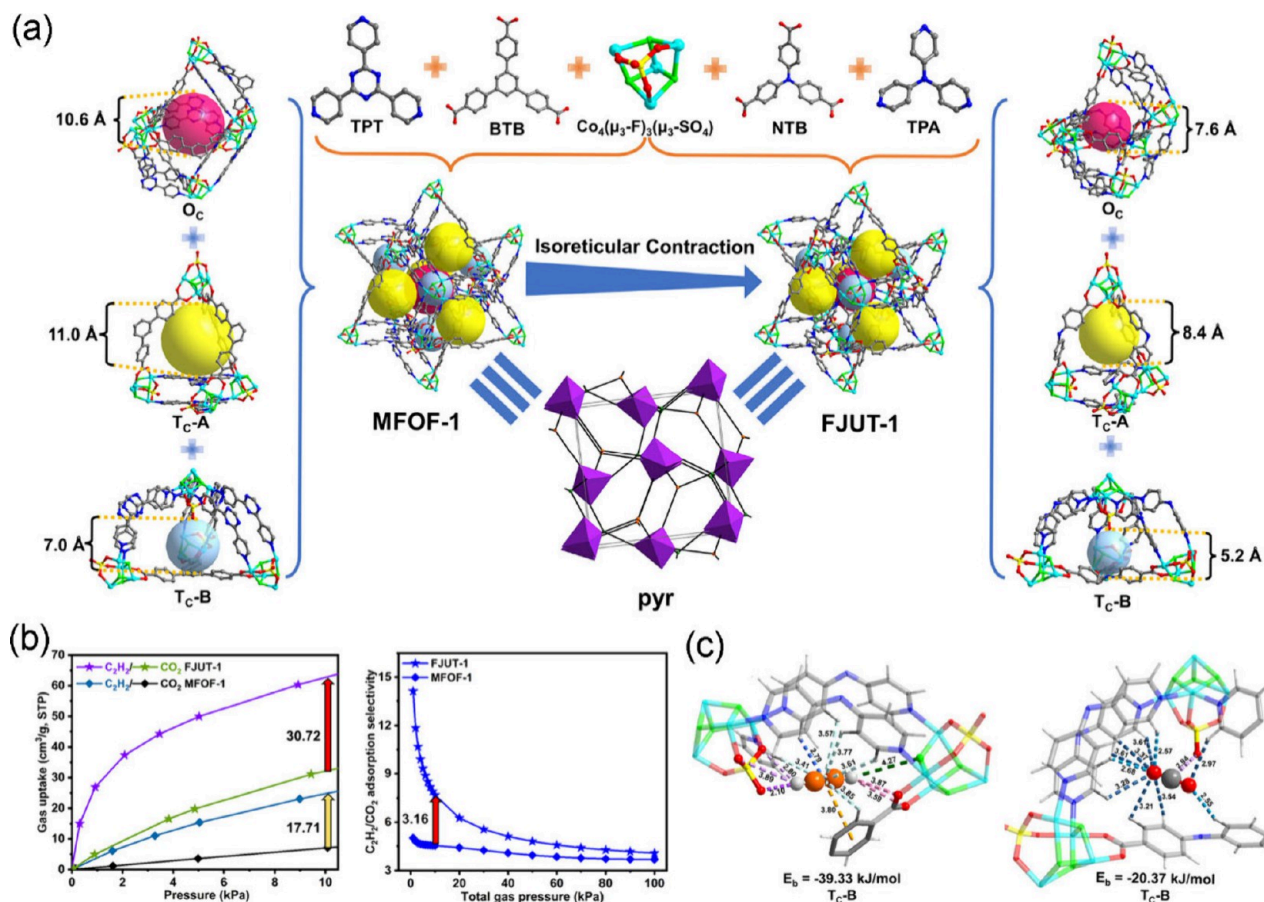


**Figure 7.** (a) Schematic illustration of nanospace engineering through the isoreticular contraction strategy in FJUT-1. (b) C<sub>2</sub>H<sub>2</sub>, CO<sub>2</sub> adsorption isotherms and IAST selectivity. (c) C<sub>2</sub>H<sub>2</sub> and CO<sub>2</sub> binding sites in FJUT-1. Reproduced with permission from ref 40. Copyright 2024 American Chemical Society.

the first time two isostructural Fe-MOFs, named LIFM-26[Fe<sup>II</sup>/Fe<sup>III</sup>] and LIFM-27[Fe<sup>III</sup>], by manipulating the electronic states of the metal centers to systematically investigate their C<sub>2</sub>H<sub>2</sub>/CO<sub>2</sub> separation performance (Figure 6).<sup>39</sup> LIFM-26 is a mixed-valent MOF containing an equal ratio of Fe<sup>II</sup>/Fe<sup>III</sup>, which exhibits a high C<sub>2</sub>H<sub>2</sub> adsorption capacity of 131 cm<sup>3</sup> g<sup>-1</sup> at 298 K and 1 bar, higher than some of the well-known MOFs such as Zn-MOF-74 (122 cm<sup>3</sup> g<sup>-1</sup>), PCP-33 (122 cm<sup>3</sup> g<sup>-1</sup>) and UTSA-74a (104 cm<sup>3</sup> g<sup>-1</sup>). In contrast, LIFM-27, which contains only Fe<sup>III</sup> sites, showed a moderate C<sub>2</sub>H<sub>2</sub> uptake of 97 cm<sup>3</sup> g<sup>-1</sup> under identical condition. To further confirm the crucial role of Fe<sup>II</sup> in enhancing the C<sub>2</sub>H<sub>2</sub> uptake capacity, another mixed-valent MOF (LIFM-27(Fe[III])-EtOH), which has a half Fe<sup>II</sup>/Fe<sup>III</sup> ratio, shows a slightly lower C<sub>2</sub>H<sub>2</sub> uptake than that of LIFM-26 but is still much higher than that of LIFM-27. These results further highlight the key role of Fe<sup>II</sup> sites and their density in improving the adsorption performance. *In-situ* IR results and molecular simulation studies confirm the presence of dual adsorption sites in LIFM-26. It was found that Fe<sup>II</sup> sites, which have a much shorter distance of 2.61 Å, interact more strongly with C<sub>2</sub>H<sub>2</sub> than do the Fe<sup>III</sup> sites. Additionally, dynamic breakthrough experiments further confirmed the excellent separation of C<sub>2</sub>H<sub>2</sub> from CO<sub>2</sub>, with a C<sub>2</sub>H<sub>2</sub> capture productivity of 60 cm<sup>3</sup> g<sup>-1</sup> for LIFM-26.

Pore space partitioning, achieved by installing suitable ligands into the larger pore spaces, is a widely recognized strategy for reducing pore size and maximizing host-guest

interactions for enhancing gas separation.<sup>51,52</sup> In this context, we recently developed an isoreticular contraction approach in cage-like MOFs for highly efficient C<sub>2</sub>H<sub>2</sub>/CO<sub>2</sub> and C<sub>2</sub>H<sub>2</sub>/C<sub>2</sub>H<sub>4</sub> separation (Figure 7).<sup>40</sup> The smaller cage cavity size and the functionalized pore surface of the compacted polyhedral cages in FJUT-1 contribute to stronger host-guest interactions through multiple supramolecular interactions (such as C-H...F and C-H...O, as observed from DFT studies). This leads to higher uptake capacities for C<sub>2</sub>H<sub>2</sub> (133.2 cm<sup>3</sup> g<sup>-1</sup>) and CO<sub>2</sub> (108.4 cm<sup>3</sup> g<sup>-1</sup>) compared to the prototypical MFOF-1 (C<sub>2</sub>H<sub>2</sub> 105.9 cm<sup>3</sup> g<sup>-1</sup> and CO<sub>2</sub> 51.5 cm<sup>3</sup> g<sup>-1</sup>) under 298 K and 100 kPa. The C<sub>2</sub>H<sub>2</sub> uptake capacity in FJUT-1 is even higher than some of the OMSs containing MOFs such as ZJU-74 (85.7 cm<sup>3</sup> g<sup>-1</sup>), JNU-2 (103 cm<sup>3</sup> g<sup>-1</sup>), NKMOF-1-Ni (61 cm<sup>3</sup> g<sup>-1</sup>) and Zn-MOF-74 (123.05 cm<sup>3</sup> g<sup>-1</sup>). Even at 10 kPa, C<sub>2</sub>H<sub>2</sub> uptake of 62.76 cm<sup>3</sup> g<sup>-1</sup> is slightly lower than that of benchmark HKUST-1 (73.78 cm<sup>3</sup> g<sup>-1</sup>) and ATC-Cu (85.79 cm<sup>3</sup> g<sup>-1</sup>). Moreover, the C<sub>2</sub>H<sub>2</sub> and CO<sub>2</sub> uptake in FJUT-1 was 2.5-fold higher than MFOF-1 (at 10 kPa), leading to a higher selectivity of 4.06 compared to 3.66 for MFOF-1, and enhanced separation potential. The real time C<sub>2</sub>H<sub>2</sub> separation performance of FJUT-1 was demonstrated in a column breakthrough study exhibiting a higher C<sub>2</sub>H<sub>2</sub> retention time than MFOF-1. The separation performance remains intact in the presence of 70% RH, and with the pH-treated material further implying its potential for real-world applications.

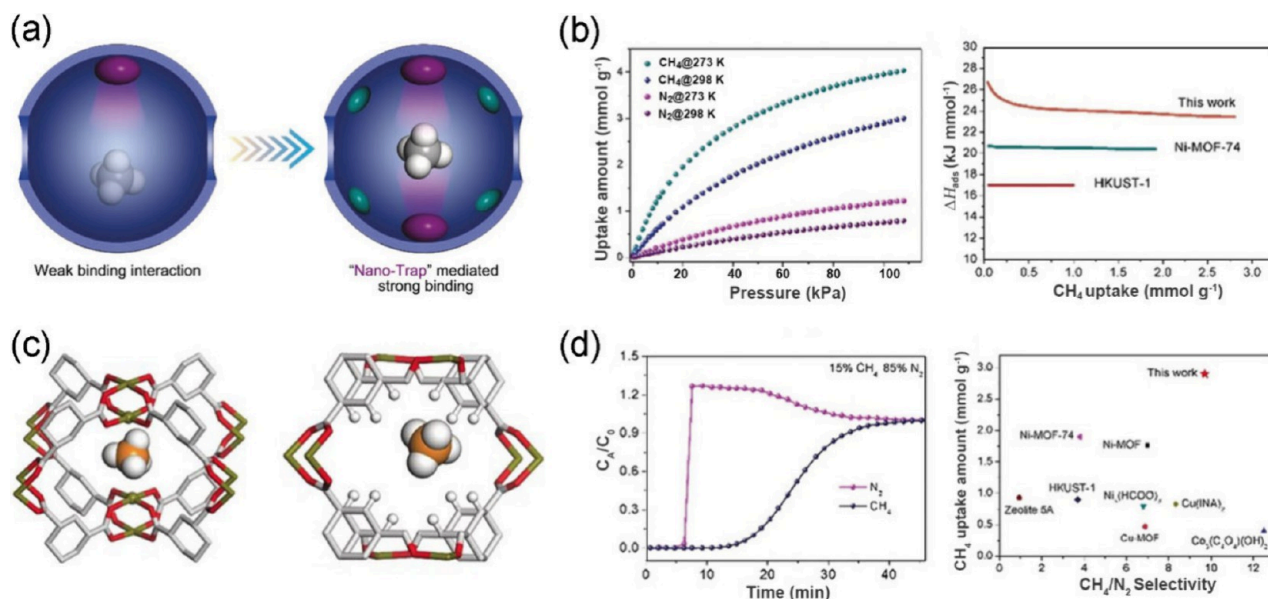


**Figure 8.** (a) Pictorial representation of binding interaction of conventional and nanotrap material. (b-d) CH<sub>4</sub> adsorption performance, simulated binding sites, and CH<sub>4</sub>/N<sub>2</sub> separation performance of ATC-Cu. Reproduced with permission from ref 42. Copyright 2019 Wiley-VCH.

#### 2.4. Incorporating Nanotraps for CH<sub>4</sub>/N<sub>2</sub> Separation

Methane (CH<sub>4</sub>) is the second largest contributor to greenhouse gases, following carbon dioxide. One of the major CH<sub>4</sub> emission sources is coal mines (known as coal mine methane, CMM), which contribute almost 70% of worldwide methane emissions.<sup>53</sup> The methane concentration in CMM varies and is typically mixed with nitrogen and other gases, making it impossible to use directly. Thus, efficient capture and separation of CMM can reduce CH<sub>4</sub> emission into the atmosphere, while also facilitating its commercial use as a clean fossil fuel and industrial raw material. Although traditional adsorbents such as zeolite and activated carbon have been employed, their inefficient performance—characterized by low selectivity and productivity—has prompted researchers to develop more effective materials for this purpose.

In 2019, we first developed a CH<sub>4</sub> nanotrap, ATC-Cu, featuring sandwich-like OMSs and dense alkyl groups for the highly efficient capture and recovery of coal mine methane (Figure 8).<sup>42</sup> At 298 K and 1 bar, ATC-Cu exhibited the highest CH<sub>4</sub> uptake (2.90 mmol g<sup>-1</sup>), surpassing all of the reported porous materials, including MOF-74-Ni (1.91 mmol g<sup>-1</sup>), Ni-MOF (1.90 mmol g<sup>-1</sup>), Zeolite-5A (0.93 mmol g<sup>-1</sup>), and HKUST-1 (0.90 mmol g<sup>-1</sup>), along with a superior heat of adsorption ( $Q_{st} = 26.8$  kJ mol<sup>-1</sup>). The single crystal structure of the CH<sub>4</sub> loaded sample further confirms the primary adsorption site as the opposite neighboring Cu<sup>II</sup> paddlewheels cavity, consistent with the molecular simulation studies. The CMM separation potential was evaluated with IAST calculation for the equimolar mixture, exhibiting an excellent selectivity of 9.7 and a record high simulated uptake of 1.86 mmol g<sup>-1</sup>, addressing both challenges of high selectivity and productivity. Furthermore, the breakthrough studies with different CH<sub>4</sub>/N<sub>2</sub> mixtures (v/v = 50/50; 30/70; 15/85), demonstrated the real separation potential for capturing CMM with low CH<sub>4</sub> concentration as a clear separation was observed for each mixture.

#### 2.5. Self-Adjusting Nanotraps and Charged Pore Surfaces for Xe/Kr Separation

Xenon (Xe) and Krypton (Kr) are valuable commodities extensively used in the electronics industry, medical imaging, spacecraft, and basic research.<sup>54</sup> Both Xe and Kr are present in the atmosphere in deficient concentrations (Xe: 0.087 ppmv; Kr: 1.14 ppmv). Such ultralow concentration makes their capture and separation highly cost-intensive. Currently, pure Xe/Kr are obtained from the cryogenic distillation of the byproduct of air separation, which typically contains 20/80 (v/v) Xe/Kr and consumes a large amount of energy. Alternative energy-efficient methods, such as adsorptive separation using MOFs, could reduce the production costs of xenon, thereby benefiting downstream industries. Inspired by strategically engineered electric fields within porous frameworks, which can induce polarization of Xe atoms and significantly enhance Xe adsorption performance.<sup>55,56</sup> In 2022, a three-dimensional cationic MOF (FJU-55, [Cu<sub>6</sub>(μ<sub>3</sub>-OH)<sub>2</sub>(CPT)<sub>8</sub>]<sub>2</sub>Br, HCPT = 4-(4H-1,2,4-triazol-4-yl)benzoic acid) was developed for low-cost, energy-efficient Xe/Kr mixture separation.<sup>41</sup> FJU-55 contains [Cu<sub>3</sub>(μ<sub>3</sub>-OH)] core which are extended by CPT ligands, resulting in a triangle-tessellated 2D structure along the *ab* plane and counter Br<sup>-</sup> provides charge neutrality. These layers are further pillared by CPT ligand, forming the 2-fold interpenetrated 3D open structure. The suitable pore size and the cationic pore surface of FJU-55 allow for significant Xe uptake at low pressure, achieving a maximum uptake of 1.41 mmol g<sup>-1</sup> (at 298 K and 1 bar) and remarkable isosteric heat of adsorption ( $Q_{st} = 39.4$  kJ mol<sup>-1</sup>). The high  $Q_{st}$  value for Xe is attributed to the enhanced interaction arising from the polarization of the electron clouds caused by the internal pore surface of the cationic framework. The breakthrough study demonstrated the practical separation potential with a dynamic Xe capture capacity of 1.3 mol kg<sup>-1</sup> and a Kr productivity of 2.2 mol kg<sup>-1</sup> without any performance loss over the cyclic study. This work demonstrates that the construction of ionic frameworks can serve as an effective strategy for the separation of inert gas mixtures.

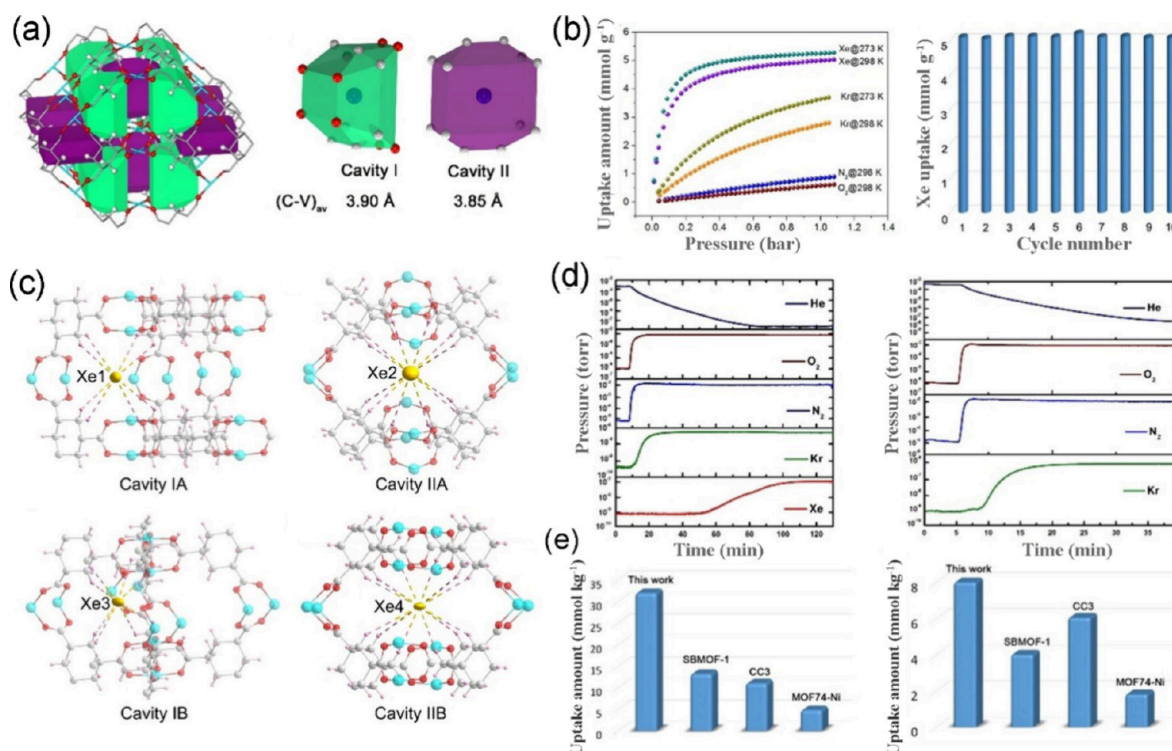


**Figure 9.** (a) Schematic representation of the cavities in ATC-Cu. (b) Xe–Kr adsorption and cycling performance. (c) Xe binding sites from single crystal structure. (d) Breakthrough separation performance with a low concentration Xe/Kr mixture. (e) Xe and Kr uptake amount comparison with top performing materials. Reproduced with permission from ref 44. Copyright 2022 Wiley-VCH.

An alternative Xe production method utilizing nuclear fission gas could serve as an effective solution considering the limited availability of atmospheric xenon. However, the waste nuclear fuel of the nuclear power plant contains radioactive xenon ( $^{135}\text{Xe}$ ) and krypton ( $^{85}\text{Kr}$ ) mixed with other species, which are difficult to separate. There is a growing demand for high-performance Xe/Kr separation materials to tackle the significant challenge of safer capture and utilization. A semirigid framework (ATC-Cu) with "nanotrap" binding sites has been developed that selectively adapts its pores under low Xe and Kr concentrations over nuclear-reprocessing off-gases (such as  $\text{N}_2$  and  $\text{O}_2$ ), enabling the trace capture and separation of Xe (Figure 9).<sup>44</sup> The 3D framework of ATC-Cu features two distinct nonpolar hydrogen-rich polyhedral cavities with a center-to-vertices distance of 3.90 Å (cavity I) and 3.85 Å (cavity II), respectively. In the presence of Xe, these cavities decrease to 3.67 and 3.75 Å smartly fitting Xe atoms through multiple strong C–H/O...Xe interactions validated from the single crystal study. A similar structural change was also observed for the Kr-loaded sample, indicating similar self-adjusting behaviors. This adaptive behavior endows one of the highest Xe uptake at 0.1 bar ( $2.65 \text{ mmol g}^{-1}$  at 298 K), which is surpassing all the top-performing MOF such as MOF–Cu–H ( $2.11 \text{ mmol g}^{-1}$ ), ECUT-60 ( $1.50 \text{ mmol g}^{-1}$ ), MOF-505 ( $1.24 \text{ mmol g}^{-1}$ ), SB-MOF-1 ( $1.09 \text{ mmol g}^{-1}$ ), and Co-squrate ( $1.09 \text{ mmol g}^{-1}$ ). Notably, at 298 K and 1 bar, the Xe uptake of ATC-Cu can reach  $5.0 \text{ mmol g}^{-1}$  (or  $0.95 \text{ g cm}^{-3}$ ), which is even higher than that of xenon hydrate ( $0.85 \text{ g cm}^{-3}$ ). The IAST selectivity for a trace xenon mixture (400 ppm of Xe, balanced with  $\text{N}_2$  or  $\text{O}_2$ ) is 66 and 109, respectively, while the selectivity for a 20/80 (v/v) Xe/Kr mixture is 13.9. These results further demonstrate the potential of ATC-Cu for the efficient capture and separation of Xe and

Kr from trace mixtures, as validated through dynamic breakthrough experiments. Notably, the dynamic adsorption capacities for ATC-Cu toward Xe and Kr are 32 and  $8 \text{ mmol kg}^{-1}$ , respectively, much higher than any benchmark porous material tested thus far.

### 3. SUMMARY AND OUTLOOK

In this Account, we summarize our recent advancements in nanospace engineering aimed at developing top-performance MOF materials for gas separation applications, ranging from light hydrocarbon purification to rare gas separation and coalbed methane enrichment. For those MOF materials, exceptional separation performance for several challenging gas mixtures was realized by fine-tuning the pore surface chemistry, spatial dimensions, geometric configurations, or combinations thereof. By virtue of the explicit single-crystal structures of MOFs, we facilitate the elucidation of separation mechanisms and structure–property relationships at the molecular level. In addition, the principles of reticular chemistry and the assembly of building blocks have enabled us to exert precise control over the pore structure and chemical composition of porous MOF materials. The remarkable potential of MOF materials with excellent adsorption performance for gas separation greatly surpasses that of conventional porous materials like zeolites and activated carbons. This advancement has exceeded the initial imagination among scientists and engineers. Consequently, the application of porous MOF materials for the separation of industrial gas mixtures is anticipated, primarily employing adsorptive separation and membrane-based technologies.

Despite the exceptional performance of numerous porous MOF materials in gas separation, there are still several challenges that need to be overcome in future research and

development to enable their practical application. Key issues include the following: (I) **Long-term Durability**: Although porous MOFs have made significant strides in stability and dynamic separation properties, there is a pressing need to evaluate their long-term cycling stability and tolerance to trace impurities such as water vapor and acidic or alkaline gases, which directly impact their feasibility for practical applications. Future research could overcome the issues by refining nanospace engineering approaches, such as leveraging the hard–soft acid–base principle to establish strong metal–ligand bonds or utilizing high-nuclearity clusters as nodes for framework construction. Moreover, incorporating hydrophobic functional groups into the pore surfaces of MOFs can substantially enhance their stability against moisture. (II) **Shaping and Mechanical Stability**: The process of shaping or pelletizing MOFs is a critical step for their practical applications; however, it may lead to a reduction in the adsorption capacity. Consequently, comprehensive investigations of the mechanical stability of MOFs are imperative. Promising approaches, including polymer compositing and chemical cross-linking, have demonstrated potential for enhancing the mechanical stability of porous materials. However, further systematic research is necessary to validate and optimize these strategies for practical applications. (III) **Economical and Scalable Synthesis**: The primary barrier to widespread commercialization of MOFs is their high synthetic cost. Therefore, it is essential to explore cost-effective synthetic pathways for large-scale production, where solvent-free and continuous synthesis methods show great potential. Additionally, equally critical is the systematic investigation of diffusion kinetics associated with MOF pellets, as it fundamentally governs both separation efficiency and energy consumption in practical applications. Although certain critical challenges stem from fundamental scientific limitations that extend beyond nanospace engineering, we posit that coordinated multi-disciplinary research efforts involving researchers, engineers, and industry stakeholders may overcome these barriers. Such synergistic partnerships have the potential to significantly enhance the application of MOF adsorbents in key industrial gas separation processes, ultimately resulting in substantial energy savings and environmental benefits.

## AUTHOR INFORMATION

### Corresponding Authors

**Yingxiang Ye** – Fujian Provincial Key Laboratory of Polymer Materials, College of Chemistry and Materials Science, Fujian Normal University, Fuzhou 350117, People's Republic of China; [orcid.org/0000-0003-3962-8463](https://orcid.org/0000-0003-3962-8463);  
Email: [yingxiangye@fjnu.edu.cn](mailto:yingxiangye@fjnu.edu.cn)

**Shengqian Ma** – Department of Chemistry, University of North Texas, Denton, Texas 76201, United States;  
[orcid.org/0000-0002-1897-7069](https://orcid.org/0000-0002-1897-7069);  
Email: [shengqian.ma@unt.edu](mailto:shengqian.ma@unt.edu)

### Authors

**Lingshan Gong** – Fujian Provincial Key Laboratory of Polymer Materials, College of Chemistry and Materials Science, Fujian Normal University, Fuzhou 350117, People's Republic of China

**Shyam Chand Pal** – Fujian Provincial Key Laboratory of Polymer Materials, College of Chemistry and Materials Science, Fujian Normal University, Fuzhou 350117, People's Republic of China

Complete contact information is available at:  
<https://pubs.acs.org/10.1021/accountsmr.5c00006>

## Author Contributions

<sup>§</sup>L.G. and S.C.P. contributed equally to this work.

## Notes

The authors declare no competing financial interest.

## Biographies

**Lingshan Gong** received her Ph.D. from South China University of Technology in 2019. After researching at Prof. Shengqian Ma's group, she joined Fujian Normal University as an associate professor in 2023. Her current research interests mainly focus on the designs and syntheses of multifunctional nanoscale porous materials and their applications in gas adsorption and theranostics of diseases.

**Shyam Chand Pal** received his M.Sc. in 2017 and obtained his Ph.D in 2023 from Indian Institute of Technology Kharagpur. Currently, he is a postdoctoral researcher at Fujian Normal University, working with Prof. Banglin Chen and Prof. Yingxiang Ye. His research interest focuses on design and synthesis of metal–organic frameworks for high-performance gas separation applications.

**Yingxiang Ye** received his Ph.D. from Fujian Normal University in 2019. In 2018–2023, he worked with Profs. Banglin Chen and Shengqian Ma, respectively. He joined Fujian Normal University as a “Minjiang Scholar” Distinguished Professor in 2023. His current research focuses on multifunctional crystalline porous framework materials and their applications in gas storage/separation, ion conduction, and fluorescent bioimaging and biosensing.

**Shengqian Ma** obtained his B.S. Degree from Jilin University (China) in 2003, and graduated from Miami University (Ohio, USA) with a PhD Degree in 2008. After finishing a two-year Director's Postdoctoral Fellowship at Argonne National Laboratory, he joined the Department of Chemistry at University of South Florida as an Assistant Professor in 2010; he was promoted to Associate Professor with early tenure in 2015 and to Full Professor in 2018. In August 2020, he joined the University of North Texas as the Robert A. Welch Chair in Chemistry. His current research interest focuses on the task-specific design and functionalization of advanced porous materials for energy-, biological-, and environmental-related applications.

## ACKNOWLEDGMENTS

The authors are grateful for financial support from the National Natural Science Foundation of China (grant nos. 22301039 and 22405043), the Fujian Provincial Department of Science and Technology (grant no. 2024J01451), and Robert A. Welch Foundation (B-0027) for this work.

## REFERENCES

- (1) Li, J.-R.; Kuppler, R. J.; Zhou, H.-C. Selective gas adsorption and separation in metal-organic frameworks. *Chem. Soc. Rev.* **2009**, *38*, 1477–1504.
- (2) Lin, R.-B.; Xiang, S.; Zhou, W.; Chen, B. Microporous Metal-Organic Framework Materials for Gas Separation. *Chem* **2020**, *6*, 337–363.
- (3) Wu, Y.; Weckhuysen, B. M. Separation and Purification of Hydrocarbons with Porous Materials. *Angew. Chem., Int. Ed.* **2021**, *60*, 18930–18949.
- (4) Sholl, D. S.; Lively, R. P. Seven chemical separations to change the world. *Nature* **2016**, *532*, 435–437.
- (5) Yang, L.; Qian, S.; Wang, X.; Cui, X.; Chen, B.; Xing, H. Energy-efficient separation alternatives: metal-organic frameworks and

- membranes for hydrocarbon separation. *Chem. Soc. Rev.* **2020**, *49*, 5359–5406.
- (6) Chu, S.; Cui, Y.; Liu, N. The path towards sustainable energy. *Nat. Mater.* **2017**, *16*, 16–22.
- (7) Reid, C. R.; Thomas, K. M. Adsorption Kinetics and Size Exclusion Properties of Probe Molecules for the Selective Porosity in a Carbon Molecular Sieve Used for Air Separation. *J. Phys. Chem. B* **2001**, *105*, 10619–10629.
- (8) Yaghi, O. M.; Li, G.; Li, H. Selective binding and removal of guests in a microporous metal-organic framework. *Nature* **1995**, *378*, 703–706.
- (9) Furukawa, H.; Cordova, K. E.; O’Keeffe, M.; Yaghi, O. M. The chemistry and applications of metal-organic frameworks. *Science* **2013**, *341*, 1230444.
- (10) Hu, Z.; Wang, Y.; Zhao, D. Modulated Hydrothermal Chemistry of Metal-Organic Frameworks. *Acc. Mater. Res.* **2022**, *3*, 1106–1114.
- (11) Liu, Y.; Wang, C.; Yang, Q.; Ren, Q.; Bao, Z. Separation of xylene isomers using metal-organic frameworks: Addressing challenges in the petrochemical industry. *Coordin. Chem. Rev.* **2025**, *523*, 216229.
- (12) Horike, S.; Kitagawa, S. The development of molecule-based porous material families and their future prospects. *Nat. Mater.* **2022**, *21*, 983–985.
- (13) Lu, W.; De Alwis Jayasinghe, D.; Schröder, M.; Yang, S. Ammonia Storage in Metal-Organic Framework Materials: Recent Developments in Design and Characterization. *Acc. Mater. Res.* **2024**, *5*, 1279–1290.
- (14) Lin, J.-B.; Nguyen, T. T. T.; Vaidhyanathan, R.; Burner, J.; Taylor, J. M.; Durekova, H.; Akhtar, F.; Mah, R. K.; Ghaffari-Nik, O.; Marx, S.; Fylstra, N.; Iremonger, S. S.; Dawson, K. W.; Sarkar, P.; Hovington, P.; Rajendran, A.; Woo, T. K.; Shimizu, G. K. H. A scalable metal-organic framework as a durable physisorbent for carbon dioxide capture. *Science* **2021**, *374*, 1464–1469.
- (15) Qian, J.; Jiang, F.; Yuan, D.; Wu, M.; Zhang, S.; Zhang, L.; Hong, M. Highly selective carbon dioxide adsorption in a water-stable indium-organic framework material. *Chem. Commun.* **2012**, *48*, 9696–9698.
- (16) Dong, A.; Chen, D.; Li, Q.; Qian, J. Metal-Organic Frameworks for Greenhouse Gas Applications. *Small* **2023**, *19*, No. e2201550.
- (17) Sengupta, D.; Melix, P.; Bose, S.; Duncan, J.; Wang, X.; Mian, M. R.; Kirlikovali, K. O.; Joodaki, F.; Islamoglu, T.; Yildirim, T.; Snurr, R. Q.; Farha, O. K. Air-Stable Cu(I) Metal-Organic Framework for Hydrogen Storage. *J. Am. Chem. Soc.* **2023**, *145*, 20492–20502.
- (18) Ren, J.; Niu, Z.; Ye, Y.; Tsai, C. Y.; Liu, S.; Liu, Q.; Huang, X.; Nafady, A.; Ma, S. Second-Sphere Interaction Promoted Turn-On Fluorescence for Selective Sensing of Organic Amines in a Tb(III)-based Macrocyclic Framework. *Angew. Chem., Int. Ed.* **2021**, *60*, 23705–23712.
- (19) Lustig, W. P.; Mukherjee, S.; Rudd, N. D.; Desai, A. V.; Li, J.; Ghosh, S. K. Metal-organic frameworks: functional luminescent and photonic materials for sensing applications. *Chem. Soc. Rev.* **2017**, *46*, 3242–3285.
- (20) Lu, K.; Aung, T.; Guo, N.; Weichselbaum, R.; Lin, W. Nanoscale Metal-Organic Frameworks for Therapeutic, Imaging, and Sensing Applications. *Adv. Mater.* **2018**, *30*, No. e1707634.
- (21) Bavykina, A.; Kolobov, N.; Khan, I. S.; Bau, J. A.; Ramirez, A.; Gascon, J. Metal-Organic Frameworks in Heterogeneous Catalysis: Recent Progress, New Trends, and Future Perspectives. *Chem. Rev.* **2020**, *120*, 8468–8535.
- (22) Li, C. N.; Liu, L.; Liu, S.; Yuan, D. Q.; Zhang, Q.; Han, Z. B. Guest Cation Functionalized Metal Organic Framework for Highly Efficient C<sub>2</sub>H<sub>2</sub>/CO<sub>2</sub> Separation. *Small* **2024**, *20*, 2405561.
- (23) Zhang, J.-P.; Liao, P.-Q.; Zhou, H.-L.; Lin, R.-B.; Chen, X.-M. Single-crystal X-ray diffraction studies on structural transformations of porous coordination polymers. *Chem. Soc. Rev.* **2014**, *43*, 5789–5814.
- (24) Peng, Y. L.; Wang, T.; Jin, C.; Deng, C. H.; Zhao, Y.; Liu, W.; Forrest, K. A.; Krishna, R.; Chen, Y.; Pham, T.; Space, B.; Cheng, P.; Zaworotko, M. J.; Zhang, Z. Efficient propyne/propadiene separation by microporous crystalline physisorbents. *Nat. Commun.* **2021**, *12*, 5768.
- (25) Xiang, S. C.; Zhang, Z.; Zhao, C. G.; Hong, K.; Zhao, X.; Ding, D. R.; Xie, M. H.; Wu, C. D.; Das, M. C.; Gill, R.; Thomas, K. M.; Chen, B. Rationally tuned micropores within enantiopure metal-organic frameworks for highly selective separation of acetylene and ethylene. *Nat. Commun.* **2011**, *2*, 204.
- (26) Cui, X.; Chen, K.; Xing, H.; Yang, Q.; Krishna, R.; Bao, Z.; Wu, H.; Zhou, W.; Dong, X.; Han, Y.; Li, B.; Ren, Q.; Zaworotko, M. J.; Chen, B. Pore chemistry and size control in hybrid porous materials for acetylene capture from ethylene. *Science* **2016**, *353*, 141–144.
- (27) Bloch, E. D.; Queen, W. L.; Krishna, R.; Zadrozny, J. M.; Brown, C. M.; Long, J. R. Hydrocarbon Separations in a Metal-Organic Framework with Open Iron(II) Coordination Sites. *Science* **2012**, *335*, 1606–1610.
- (28) Lin, R. B.; Li, L.; Zhou, H. L.; Wu, H.; He, C.; Li, S.; Krishna, R.; Li, J.; Zhou, W.; Chen, B. Molecular sieving of ethylene from ethane using a rigid metal-organic framework. *Nat. Mater.* **2018**, *17*, 1128–1133.
- (29) Li, L.; Lin, R. B.; Krishna, R.; Li, H.; Xiang, S.; Wu, H.; Li, J.; Zhou, W.; Chen, B. Ethane/ethylene separation in a metal-organic framework with iron-peroxo sites. *Science* **2018**, *362*, 443–446.
- (30) Cadiau, A.; Adil, K.; Bhatt, P. M.; Belmabkhout, Y.; Eddaoudi, M. A metal-organic framework-based splitter for separating propylene from propane. *Science* **2016**, *353*, 137–140.
- (31) Tian, Y. J.; Deng, C. H.; Zhao, L.; Zou, J. S.; Wu, X. C.; Jia, Y. N.; Zhang, Z. Y.; Zhang, J.; Peng, Y. L.; Chen, G. J.; Zaworotko, M. J. Pore configuration control in hybrid azolate ultra-microporous frameworks for sieving propylene from propane. *Nat. Chem.* **2025**, *17*, 141–147.
- (32) Zeng, H.; Xie, M.; Wang, T.; Wei, R. J.; Xie, X. J.; Zhao, Y.; Lu, W.; Li, D. Orthogonal-array dynamic molecular sieving of propylene/propane mixtures. *Nature* **2021**, *595*, 542–548.
- (33) Li, B.; Zhang, Y.; Krishna, R.; Yao, K.; Han, Y.; Wu, Z.; Ma, D.; Shi, Z.; Pham, T.; Space, B.; Liu, J.; Thallapally, P. K.; Liu, J.; Chrzanowski, M.; Ma, S. Introduction of  $\pi$ -Complexation into Porous Aromatic Framework for Highly Selective Adsorption of Ethylene over Ethane. *J. Am. Chem. Soc.* **2014**, *136*, 8654–8660.
- (34) Zhang, Y.; Li, B.; Krishna, R.; Wu, Z.; Ma, D.; Shi, Z.; Pham, T.; Forrest, K.; Space, B.; Ma, S. Highly selective adsorption of ethylene over ethane in a MOF featuring the combination of open metal site and  $\pi$ -complexation. *Chem. Commun.* **2015**, *51*, 2714–2717.
- (35) Ye, Y.; Xie, Y.; Shi, Y.; Gong, L.; Phipps, J.; Al-Enizi, A. M.; Nafady, A.; Chen, B.; Ma, S. A Microporous Metal-Organic Framework with Unique Aromatic Pore Surfaces for High Performance C<sub>2</sub>H<sub>6</sub>/C<sub>2</sub>H<sub>4</sub> Separation. *Angew. Chem., Int. Ed.* **2023**, *62*, No. e202302564.
- (36) Chen, C. X.; Wei, Z. W.; Pham, T.; Lan, P. C.; Zhang, L.; Forrest, K. A.; Chen, S.; Al-Enizi, A. M.; Nafady, A.; Su, C. Y.; Ma, S. Nanospace Engineering of Metal-Organic Frameworks through Dynamic Spacer Installation of Multifunctionalities for Efficient Separation of Ethane from Ethane/Ethylene Mixtures. *Angew. Chem., Int. Ed.* **2021**, *60*, 9680–9685.
- (37) Wang, X.; Niu, Z.; Al-Enizi, A. M.; Nafady, A.; Wu, Y.; Aguila, B.; Verma, G.; Wojtas, L.; Chen, Y.-S.; Li, Z.; Ma, S. Pore environment engineering in metal-organic frameworks for efficient ethane/ethylene separation. *J. Mater. Chem. A* **2019**, *7*, 13585–13590.
- (38) Ye, Y.; Xian, S.; Cui, H.; Tan, K.; Gong, L.; Liang, B.; Pham, T.; Pandey, H.; Krishna, R.; Lan, P. C.; Forrest, K. A.; Space, B.; Thonhauser, T.; Li, J.; Ma, S. Metal-Organic Framework Based Hydrogen-Bonding Nanotrap for Efficient Acetylene Storage and Separation. *J. Am. Chem. Soc.* **2022**, *144*, 1681–1689.
- (39) Chen, C.-X.; Pham, T.; Tan, K.; Krishna, R.; Lan, P. C.; Wang, L.; Chen, S.; Al-Enizi, A. M.; Nafady, A.; Forrest, K. A.; Wang, H.; Wang, S.; Shan, C.; Zhang, L.; Su, C.-Y.; Ma, S. Regulating C<sub>2</sub>H<sub>2</sub>/CO<sub>2</sub> adsorption selectivity by electronic-state manipulation of iron in metal-organic frameworks. *Cell Rep. Phys. Sci.* **2022**, *3*, 100977.

(40) Zhang, L.; Xiao, T.; Zeng, X.; You, J.; He, Z.; Chen, C.-X.; Wang, Q.; Nafady, A.; Al-Enizi, A. M.; Ma, S. Isoreticular Contraction of Cage-like Metal-Organic Frameworks with Optimized Pore Space for Enhanced  $C_2H_2/CO_2$  and  $C_2H_2/C_2H_4$  Separations. *J. Am. Chem. Soc.* **2024**, *146*, 7341–7351.

(41) Gong, L.; Liu, Y.; Ren, J.; Al-Enizi, A. M.; Nafady, A.; Ye, Y.; Bao, Z.; Ma, S. Utilization of cationic microporous metal-organic framework for efficient Xe/Kr separation. *Nano Res.* **2022**, *15*, 7559–7564.

(42) Niu, Z.; Cui, X.; Pham, T.; Lan, P. C.; Xing, H.; Forrest, K. A.; Wojtas, L.; Space, B.; Ma, S. A Metal-Organic Framework Based Methane Nano-trap for the Capture of Coal-Mine Methane. *Angew. Chem., Int. Ed.* **2019**, *58*, 10138–10141.

(43) Niu, Z.; Cui, X.; Pham, T.; Verma, G.; Lan, P. C.; Shan, C.; Xing, H.; Forrest, K. A.; Suepaul, S.; Space, B.; Nafady, A.; Al-Enizi, A. M.; Ma, S. A MOF-based Ultra-Strong Acetylene Nano-trap for Highly Efficient  $C_2H_2/CO_2$  Separation. *Angew. Chem., Int. Ed.* **2021**, *60*, 5283–5288.

(44) Niu, Z.; Fan, Z.; Pham, T.; Verma, G.; Forrest, K. A.; Space, B.; Thallapally, P. K.; Al-Enizi, A. M.; Ma, S. Self-Adjusting Metal-Organic Framework for Efficient Capture of Trace Xenon and Krypton. *Angew. Chem., Int. Ed.* **2022**, *61*, No. e202117807.

(45) Gao, Y.; Neal, L.; Ding, D.; Wu, W.; Baroi, C.; Gaffney, A. M.; Li, F. Recent Advances in Intensified Ethylene Production—A Review. *ACS Catal.* **2019**, *9*, 8592–8621.

(46) Uchida, S.; Kawamoto, R.; Tagami, H.; Nakagawa, Y.; Mizuno, N. Highly Selective Sorption of Small Unsaturated Hydrocarbons by Nonporous Flexible Framework with Silver Ion. *J. Am. Chem. Soc.* **2008**, *130*, 12370–12376.

(47) Lv, D.; Zhou, P.; Xu, J.; Tu, S.; Xu, F.; Yan, J.; Xi, H.; Yuan, W.; Fu, Q.; Chen, X.; Xia, Q. Recent advances in adsorptive separation of ethane and ethylene by  $C_2H_4$ -selective MOFs and other adsorbents. *Chem. Eng. J.* **2022**, *431*, 133208.

(48) Han, X.; Yang, S. H. Molecular Mechanisms behind Acetylene Adsorption and Selectivity in Functional Porous Materials. *Angew. Chem., Int. Ed.* **2023**, *62*, No. e202218274.

(49) Matsuda, R.; Kitaura, R.; Kitagawa, S.; Kubota, Y.; Belosludov, R. V.; Kobayashi, T. C.; Sakamoto, H.; Chiba, T.; Takata, M.; Kawazoe, Y.; Mita, Y. Highly controlled acetylene accommodation in a metal-organic microporous material. *Nature* **2005**, *436*, 238–241.

(50) Zhang, L.; Li, F.; You, J.; Hua, N.; Wang, Q.; Si, J.; Chen, W.; Wang, W.; Wu, X.; Yang, W.; Yuan, D.; Lu, C.; Liu, Y.; Al-Enizi, A. M.; Nafady, A.; Ma, S. A window-space-directed assembly strategy for the construction of supertetrahedron-based zeolitic mesoporous metal-organic frameworks with ultramicroporous apertures for selective gas adsorption. *Chem. Sci.* **2021**, *12*, 5767–5773.

(51) Hong, A. N.; Yang, H.; Bu, X.; Feng, P. Pore space partition of metal-organic frameworks for gas storage and separation. *EnergyChem.* **2022**, *4*, 100080.

(52) Ye, Y.; Ma, Z.; Lin, R. B.; Krishna, R.; Zhou, W.; Lin, Q.; Zhang, Z.; Xiang, S.; Chen, B. Pore Space Partition within a Metal-Organic Framework for Highly Efficient  $C_2H_2/CO_2$  Separation. *J. Am. Chem. Soc.* **2019**, *141*, 4130–4136.

(53) Yang, J.; Liu, J.; Liu, P.; Li, L.; Tang, X.; Shang, H.; Li, J.; Chen, B. K-Chabazite Zeolite Nanocrystal Aggregates for Highly Efficient Methane Separation. *Angew. Chem., Int. Ed.* **2022**, *61*, No. e202116850.

(54) Banerjee, D.; Cairns, A. J.; Liu, J.; Motkuri, R. K.; Nune, S. K.; Fernandez, C. A.; Krishna, R.; Strachan, D. M.; Thallapally, P. K. Potential of metal-organic frameworks for separation of xenon and krypton. *Acc. Chem. Res.* **2015**, *48*, 211–219.

(55) Liu, J.; Strachan, D. M.; Thallapally, P. K. Enhanced noble gas adsorption in  $Ag@MOF-74Ni$ . *Chem. Commun.* **2014**, *50*, 466–468.

(56) Liu, B.; Gong, Y.; Wu, X.; Liu, Q.; Li, W.; Xiong, S.; Hu, S.; Wang, X. Enhanced xenon adsorption and separation with an anionic indium-organic framework by ion exchange with  $Co^{2+}$ . *RSC Adv.* **2017**, *7*, 55012–55019.